



# A comprehensive study on the effect of small rates of walnut shell and talc fillers on the thermal, mechanical, and morphological properties of epoxy hybrid composites

İdris Karagöz<sup>1</sup> · Derya Mutlu<sup>2</sup> · Aysu Çavuşoğlu<sup>2</sup> · Mithat Çelebi<sup>1</sup> · Özgür Ceylan<sup>3</sup>

Received: 29 January 2024 / Revised: 28 March 2024 / Accepted: 19 April 2024 / Published online: 7 May 2024  
© The Author(s) 2024

## Abstract

Epoxy-based composites, valued for their cost-effectiveness and remarkable mechanical properties, attract considerable attention from researchers in academia and industry. This study explores the impact of low concentrations (1% to 3%) of walnut shell (WS) and talc additives on the density, water absorption, and mechanical (tensile, three-point bending, impact, hardness) as well as thermal (TGA, DSC) properties of epoxy composites. While prior research has extensively covered epoxy composites with high concentrations of walnut shell and talc, their utilization in lower concentrations remains under-explored. Findings highlight the substantial influence of incorporating low percentages of walnut shell and talc on the T<sub>g</sub> temperatures of epoxy composites, with talc reducing T<sub>g</sub> temperature and WS elevating it. TGA tests reveal that both WS and talc contribute to increased T<sub>max</sub> temperature and residue content compared to pure epoxy. Mechanical properties exhibit variations based on filler type and amount, with walnut shell enhancing the elastic modulus and talc decreasing it compared to pure epoxy. Impact resistance sees significant reductions related to particle size. Talc boosts density, while WS has a more pronounced effect on hardness. Water absorption tests demonstrate higher water absorption in WS-containing epoxy composites. Glossiness and surface roughness undergo changes, with talc increasing roughness and decreasing glossiness. In conclusion, even minor filler percentages noticeably impact epoxy composite properties compared to pure epoxy, providing avenues for customized modifications, particularly with challenging or costly fillers, offering viable alternatives for researchers in diverse fields.

**Keywords** Epoxy hybrid composites · Talc · Walnut shell · Epoxy composites

## 1 Introduction

In recent years, substantial advancements in materials science and engineering have led to the emergence of innovative composite materials endowed with superior properties compared to their conventional counterparts. Exploring the combination of epoxy resins with various fillers holds great

potential for significantly enhancing performance across a diverse spectrum of industrial applications [1] Epoxy resins find widespread use in diverse applications owing to their exceptional blend of properties, encompassing outstanding mechanical strength, high thermal stability, good chemical resistance, and exceptional electrical insulation [2] The integrity, longevity, and efficiency of engineered structural components are contingent upon the performance of their constituent materials. Industries such as aerospace, automotive, civil, and energy demand high-performance, cost-effective designs. Epoxy-based composites stand out due to their impressive strength-to-weight ratio, compatibility with diverse curing techniques, and remarkable thermal, mechanical, electrical, and chemical properties. However, their intrinsic fragility and significant expenses often constrain their broader application. To surmount these limitations, researchers have delved into integrating various additives and reinforcements into epoxy matrices [3–5].

✉ İdris Karagöz  
idris.karagoz@yalova.edu.tr

<sup>1</sup> Department of Polymer Materials Engineering, Faculty of Engineering, Yalova University, Yalova 77200, Turkey

<sup>2</sup> Department of Polymer Materials Engineering, Institute of Graduate Studies, Yalova University, 77200 Yalova, Turkey

<sup>3</sup> Yalova University Central Research Laboratory, Yalova University, Yalova 77200, Turkey

Agricultural waste products, serving as natural fillers, have garnered significant attention due to their sustainability, widespread availability, and potential for enhanced qualities [6–8]. Easily obtained as a byproduct of the walnut processing sector, walnut shells present an attractive option as a natural additive for epoxy resins, offering the potential to enhance the mechanical qualities of the composite material through their high cellulose content and natural hardness [9–11]. Consisting of 60% kernel and 40% shell, walnut shells, derived from dried walnuts, contain substantial amounts of lignin, hemicellulose, and cellulose. Pyrolysis provides a viable method to convert the shell waste, rich in lignocellulose, for heating and energy generation. Walnut shells, therefore, serve effectively as a bio-filler material [12]. The growing respect for walnut shells stems from their role in promoting the use of sustainable resources and maintaining biodiversity [13]. In a study by Salasinska et al. [9], the use of ground walnut shells as organic waste fillers to modify epoxy composites was investigated. The researchers found that while the addition of a high amount of walnut shells resulted in enhanced rigidity and hardness, it simultaneously reduced tensile strength and resistance to impact.

Talc is widely employed in various industrial applications owing to its impressive thermal and mechanical properties [14]. According to Tomasi's findings [15], the incorporation of talc into cycloaliphatic epoxy composites enhances their tensile modulus and thermal conductivity, with minimal impact on electrical resistivity. Talc offers various additional advantages that render it a compelling choice for filler substances. Initially, talc exhibits exceptional thermal resistance, making it well suited for applications involving elevated temperatures. This inherent quality ensures the stability and non-degradation of the filler material, even under intense heat conditions. Talc also demonstrates outstanding chemical inertness, indicating its resistance to chemical reactions and its aversion to undesirable chemical changes. This characteristic is crucial in situations where the filler material must preserve its integrity and avoid undesirable reactions with other materials [16]. However, walnut shells may lack sufficient thermal resistance, limiting their application in certain industries. Therefore, this investigation employed a combination of talc and walnut shell.

The aim of this study is to analyze the thermal, mechanical, and morphological characteristics of epoxy resins that have been enriched with walnut shells and talc minerals. While walnut shells hold promise as epoxy fillers, there is currently a limited understanding of their impact on the thermal, mechanical, and morphological qualities of the resulting composite materials. This study seeks to fill this gap by examining how varying amounts of walnut shell and talc filler content influence the thermal, mechanical, and morphological properties of epoxy resins.

## 2 Experimental

### 2.1 Materials and methods

In F 4000A) and curing agent (ERA 4000B) purchased from Teknomarin Inc. were used as the matrix material. The density of the two-component, solvent-free epoxy used in the study is 1.1 g/cm<sup>3</sup>, with an application range of + 15 to + 35 °C, and the recommended filler usage rate is a maximum of 7% by weight. The gel time of the filled resin after the homogenization process is 20 min. It is utilized in various fields such as wood coating, automobile steering and interior trim part coatings, and boat and caravan repairs.

The walnut shells used in the study were obtained from locally sourced Marash 18 variety walnuts (Kahramanmaraş, Çağlayancerit). The specific gravity of walnut shells ranges between 1.0 and 1.2 g/cm<sup>3</sup>, with a particle size of 250 microns. Their hardness varies between 2.5 and 3.5 on the Mohs scale. The composition of walnut shells includes 38.4% lignin, 23% cellulose, and 29% hemicellulose. WS were dried in an oven at 100 °C for 1 h before composite production. The talc used in the lamellar structure of the study has a density of 2.73 g/ml (ISO787/10) and a particle size less than 44 microns. The chemical composition of the talc used is provided in Table 1.

Talc and walnut shells were used as fillers in the epoxy matrix at varying weight percentages of 1%, 1.5%, 2%, and 3%. Talc and walnut shell particles were initially dispersed in the epoxy matrix using a mechanical mixer (Vortex Genie 2) and then homogenized with a sonicator (Sonics VCX 130). Following the homogenization process, the epoxy composite resin mixture was poured into a silicone mold (200 × 200 × 25 mm) with cavities corresponding to the shapes of the samples. After the casting process, the samples were left in the mold at room temperature for 24 h to complete the curing process. Once cured, the samples were removed from the mold. Formulation of epoxy-based composites containing walnut shell and talc, for which post-production sample visuals are provided in Fig. 1, is presented in Table 2.

**Table 1** Chemical composition of talc [17]

Component	Content (%)
MgO	32
SiO <sub>2</sub>	62
CaO	1.8 (max)
Al <sub>2</sub> O <sub>3</sub>	0.3
Fe <sub>2</sub> O <sub>3</sub>	0.6 (max)
A. Z	4

**Fig. 1** Appearance of pure epoxy, walnut shell, and talc-filled epoxy composites



**Table 2** Formulation of epoxy-based composite incorporating walnut shells and talc particles

Sample codes	Epoxy (wt.%)	Curing agent (wt.%)	Walnut shell (wt.%)	Talc (wt.%)
Pure Epoxy	66.67	33.33	–	–
E97WS3	64.66	32.33	3.0	–
E97T3	64.66	32.33	–	3.0
E97WS1T2	64.66	32.33	1.0	2.0
E97WS2T1	64.66	32.33	2.0	1.0
E97WS1.5T1.5	64.66	32.33	1.5	1.5

## 2.2 FT-IR, DSC, and TG analyses

FT-IR tests were conducted using a Thermo Scientific brand and Nicolet IS50 model device in accordance with the ASTM D6348 standard. Fourier transform infrared (FT-IR) spectroscopy was employed to analyze the chemical structures of epoxy composites, which were reinforced with different proportions of walnut shell and talc powder. This examination involved identifying peaks corresponding to functional groups within the wave number range of  $4000\text{ cm}^{-1}$  to  $400\text{ cm}^{-1}$ .

To investigate thermal properties, differential scanning calorimetry (DSC) was conducted using a DSC, Seiko DSC 7020 model, following the ASTM D3417 standard. The heating rate was set to  $10\text{ }^{\circ}\text{C}/\text{min}$ , and thermal transitions were observed under a nitrogen atmosphere to prevent the samples from burning or oxidizing during the test

at high temperatures. This helped to ensure the accuracy of the calorimetric analysis and improve sensitivity.

Thermogravimetric analysis (TGA) was performed using a Seiko Exstar TG/DTA 6300 model device under a nitrogen flow. The epoxy composite samples underwent heating up to  $600\text{ }^{\circ}\text{C}$  at a rate of  $10\text{ }^{\circ}\text{C}/\text{min}$ .

## 2.3 Mechanical examination

The tensile and flexural properties of the materials were evaluated using a Zwick Z020 model testing machine equipped with a 20-kN load cell. Tensile testing followed DIN EN ISO 527–1 standards, with a test speed of  $5\text{ mm}/\text{min}$  at room temperature. The flexural test was conducted under room temperature conditions using the same machine, adhering to ASTM D790 standards, with a span-to-depth ratio of 16:1 and a crosshead speed of  $2\text{ mm}/\text{min}$ . Additionally, an Izod impact test was performed using a pendulum universal impact tester compliant with ASTM D256, featuring a 2.5-J pendulum hammer. Each sample underwent 10 impact measurements, and both tensile and flexural tests were repeated five times.

## 2.4 Density and hardness measurements

The density of both the pure epoxy and the epoxy/WS/talc composites was determined using the liquid pycnometer method in accordance with ISO 1183 standards. To assess hardness, a Shore D scale and a Zwick Roel device were utilized, following the guidelines outlined in the ASTM D2240 standard. Each sample underwent five density

measurements, and hardness measurements were repeated 10 times.

## 2.5 Water absorption test

The pH value of the water used in the water absorption test was measured as 7.03 using the Hanna brand HI 2210 model device. The weights of samples, cut into rectangular shapes measuring  $4 \times 20 \times 30$  mm for the water absorption test, were initially measured. Subsequently, the samples were immersed in water within a test container to undergo the water absorption process. After an initial 1-h period, the materials were extracted from the container using tweezers. Excess water on the sample surfaces was removed through a drying process with paper towels, avoiding any applied pressure. Following this, the samples were reweighed, and the water absorption was calculated using the equation provided in Eq. (1) below. The same procedures were repeated at intervals ranging from 1 to 240 h.

$$\text{Water absorption capacity} = \left( \frac{\text{Finalweight} - \text{Initialweight}}{\text{Initialweight}} \right) \times 100 \quad (1)$$

## 2.6 Epoxy composites' surface quality measurement

Surface roughness measurements were conducted following ISO class 3 standards using a Mitech MR200 (Onalgon) surface roughness measuring device. The measurements were performed with an Rz measurement range of 0.1–50  $\mu\text{m}$ , employing a 1.0 mm/s feed rate, 0.4 mN load, and a diamond detector tip with a 5- $\mu\text{m}$  diameter. Surface gloss measurements were conducted using an Elcometer micro glossmeter at a 60° projection angle in accordance with ISO 2813 standard. Gloss measurements were taken from the upper surface of parts, disregarding the mold surface.

## 2.7 Microstructure characterization

A scanning electron microscope (SEM, Zeiss/Supra 40 VP) was used for microstructure characterization to examine the dispersion of WS and talc particles within the epoxy matrix and the morphology of the fracture surface. Before examination, a thin layer of gold was applied to the samples using a sputter coater (Leica EM ACE200) to enhance electron conduction and minimize charging effects. Subsequently, the samples were observed under high vacuum conditions to ensure optimal image quality. This microstructural analysis provided a deeper insight into the distribution of WS and talc particles within the epoxy matrix and their impact on the fracture behavior of the composites.

## 3 Results and discussion

### 3.1 FT-IR analyses

The FT-IR spectra of epoxy resin modified with talc and walnut shell epoxy composites are depicted in Fig. 2. The broad bands observed between 3341 and 3292  $\text{cm}^{-1}$  correspond to O–H stretching. Peaks at 2922 and 2853  $\text{cm}^{-1}$  represent the symmetric and asymmetric C–H stretching of –CH<sub>2</sub> and –CH<sub>3</sub> groups [18]. Peaks at 1608, 1508, 1457, and 1455  $\text{cm}^{-1}$  are attributed to aromatic C=C stretching. A peak observed at 1744  $\text{cm}^{-1}$  in walnut shell-filled epoxy composites, absent in pure epoxy, corresponds to the C=O stretching vibration of ester carbonyl groups in hemicellulose and pectin within the walnut shell [19]. Peaks at 1237 and 1244  $\text{cm}^{-1}$  correspond to asymmetric aromatic C–O stretching, while peaks at 1018 and 1035  $\text{cm}^{-1}$  correspond to symmetric aromatic C–O stretching [20]. The peak at 826  $\text{cm}^{-1}$  corresponds to out-of-plane aromatic –CH deformation. In summary, the FTIR spectra of pure epoxy and walnut shell-filled epoxy composites exhibit similar behavior, displaying identical peaks. In the FTIR spectrum of talc, peaks at 3658  $\text{cm}^{-1}$  and 3673  $\text{cm}^{-1}$  are attributed to vibrations of hydroxyl groups associated with Si (Si–OH) and Mg (Mg–OH), respectively. The strong band observed around 983  $\text{cm}^{-1}$  corresponds to the out-of-plane symmetric stretching of Si–O–Si groups in talc. Another sharp absorption at 675  $\text{cm}^{-1}$  originates from the stretching vibration of Si–O–Mg in the talc structure. The three bands at 1435  $\text{cm}^{-1}$  (strong), 875  $\text{cm}^{-1}$  (shoulder), and 728  $\text{cm}^{-1}$  (weak) correspond to the characteristic CO<sub>3</sub> vibration of calcite [20]. The presence of characteristic peaks of talc alongside those of epoxy resin confirms the talc content in epoxy composites containing talc.

### 3.2 DSC analyses

The DSC graphs obtained for the binary system, epoxy, and epoxy composites are shown in Fig. 3. In the pure epoxy sample, the T<sub>g</sub> value has been determined as 89.4 °C. This value indicates that the epoxy resin system is suitable for long-term applications requiring thermal stability. Epoxy systems with high T<sub>g</sub> are generally known for their durability, making them suitable for industrial applications under mechanical stress [18]. In the E97T3 sample, the T<sub>g</sub> value was determined as 88.6 °C with the addition of talc. This suggests that the inclusion of talc has slightly reduced the thermal behavior of the epoxy composite, resulting in a lower T<sub>g</sub> and a tendency for the material to become more flexible at lower temperatures. The plate-like structure of talc may have increased particle

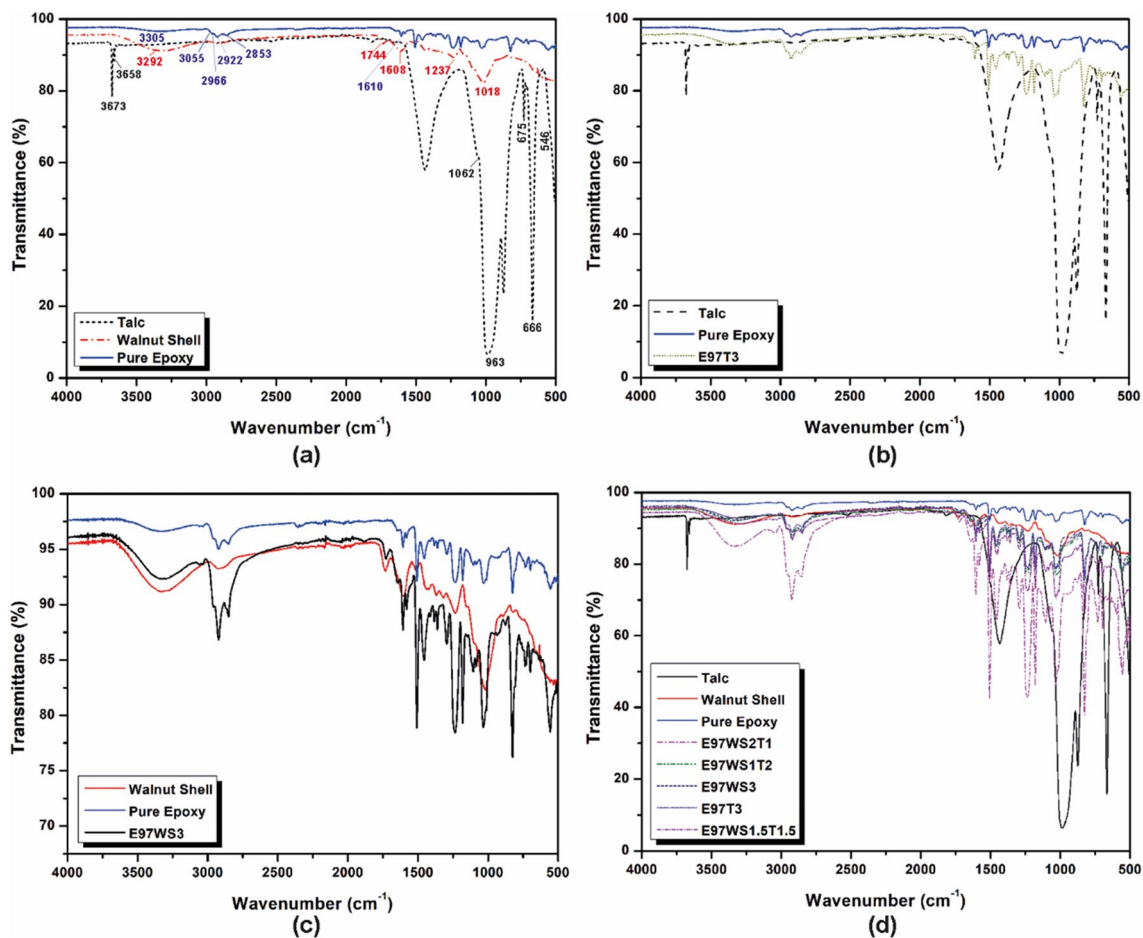
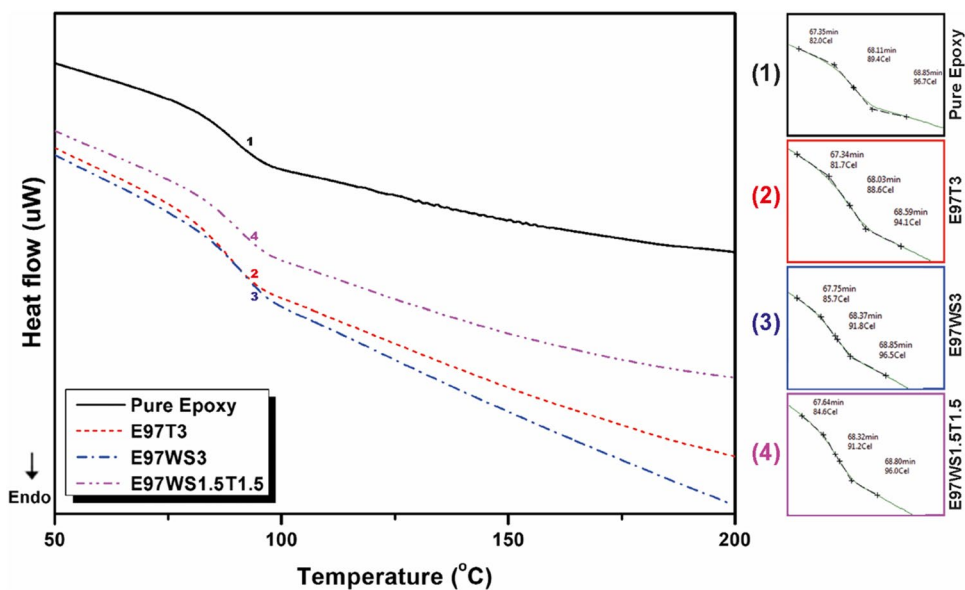


Fig. 2 Important peaks in the FT-IR spectra of epoxy and epoxy-talc-walnut shell composites in the range of 500–4000  $\text{cm}^{-1}$

Fig. 3 DSC curves: 1) pure epoxy, 2) 3% talc filled epoxy composite with code E97T3, 3) 3% WS filled epoxy composite with code E97WS3, and 4) 1.5% WS and 1.5% talc filled epoxy composite with code E97WS1.5T1.5



roughness and provided lubrication within the epoxy, contributing to a reduction in viscosity and making the material more fluid [21] This effect becomes evident in the epoxy-talc composite at the onset temperature of  $T_g$ , which is observed to be slightly lower compared to the pure epoxy system. This influence is observed across all talc loading percentages and can be attributed to oxygen-containing groups on talc molecules that can activate the epoxy ring and accelerate the reaction of epoxy with the amine [22] Moreover, talc, known for its good thermal conductivity, may have enhanced heat transfer within the material. However, based on the DSC results, this effect appears to be relatively limited.

In the E97WS3 sample, the  $T_g$  value was determined as 91.8 °C with the addition of walnut shell. Here, the higher  $T_g$  indicates a tendency for the material to become more rigid and solid at higher temperatures. This phenomenon may be influenced by the presence of cellulose in WS. The walnut shell within the composite structure might enhance the thermal stability of the material by restricting the movement of polymer chains, consequently raising the  $T_g$  temperatures by reducing heat conduction within the structure [18] Now, considering the E97WS1.5T1.5 sample, where both walnut shell and talc are used together, the  $T_g$  value is determined as 91.2 °C. This  $T_g$  value falls between the individual values obtained for E97T3 and E97WS3. The combination of walnut shell and talc seems to have a synergistic effect, resulting in a balanced  $T_g$ . This suggests that the material may exhibit a desirable combination of flexibility and rigidity, making it versatile for applications with varying temperature requirements. By comparing all four cases, it is evident that the choice and combination of additives significantly impact the  $T_g$  of the epoxy composites. These data highlight the potential to tailor the thermal behavior of

doped epoxy composites according to specific application needs.

Due to the consistent  $T_g$  changes observed in the specimens coded as E97T3, E97WS3, and E97WS1.5T1.5, and their alignment with the expected  $T_g$  temperature changes, the DSC test was not conducted on specimens coded as E97WS1T2 and E97WS2T1. It is expected that the  $T_g$  temperature for these specimens will exhibit similar behavior to E97T3 for composites with a high talc content and E97WS3 for composites with a high walnut shell content.

### 3.3 TGA analyses

The thermal stability of both pure epoxy and epoxy composites is depicted in Fig. 4, with corresponding numerical values of the TGA test results provided in Table 3. All samples demonstrate two main stages of decomposition throughout the process, taking place between 100–350 °C and 350–500 °C. In the first stage of weight loss curves (100 °C to 350 °C), the cured epoxy network undergoes degradation, resulting in approximately a 17% weight loss. In the second stage (350 °C to 500 °C), the remaining components of the cured epoxy network decompose, leading to a more substantial weight loss of around 75%. The addition of WS positively influences the thermal stability of epoxy/

**Table 3** The numerical data obtained from the TGA test

Code	$T_5$ (°C)	$T_{50}$ (°C)	$T_{max}$ (°C)	Residue at 600 °C (%)
Pure epoxy	352.1	378.1	408.9	8.2
E97T3	350.4	377.2	419.6	10.1
E97WS3	353.2	375.7	465.6	8.4
E97WS1.5T1.5	347.4	379.3	419.3	9.0

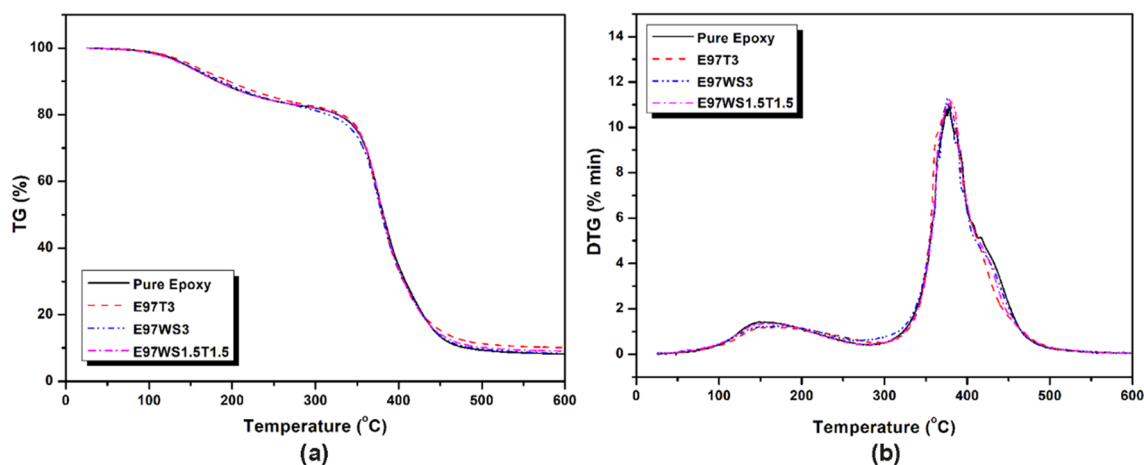


**Fig. 4** Thermogravimetric analysis (TGA) curves showing weight loss over temperature

WS composites, evident in the rightward (higher) shift of the temperature of weight loss compared to pure epoxy. This slight difference can be attributed to the interaction between the total cellulose content of WS and epoxy components, altering the material's rheology and constraining the movement of polymer chains. Overall, an increase in the WS ratio enhances thermal stability and the amount of solid residue compared to pure epoxy (residue at 600 °C). The lower T50 temperature in epoxy composites containing WS, compared to pure epoxy, might originate from the pyrolysis of cellulose content [23, 24]. The thermal decomposition of lignin components could also contribute to the increase in Tmax temperature [24]. This is because WS's passive pyrolysis region begins after 400 °C [12]. The presence of talc further increases the amount of residue in the structure compared to pure epoxy and WS contributions. Talc's high thermal conductivity and endothermic characteristics may influence T5 and T50 temperatures [21, 22].

### 3.4 Mechanical tests

The numerical values of the mechanical test results are presented in Table 4. Fig. 5a, b, and c respectively, illustrates graphs corresponding to the tensile, flexural, and Izod impact tests. Based on the tensile test results, pure epoxy demonstrated higher strength compared to epoxy composites containing talc and WS additives. The addition of talc to the epoxy structure further decreased the tensile strength compared to the WS additive. Talc exhibited a more pronounced negative impact on tensile strength compared to WS. In epoxy composites where talc and WS are used together, the increase in the WS ratio is associated with a corresponding rise in tensile strength, clearly demonstrating this effect. When comparing the impact of WS and talc on epoxy composites in terms of tensile modulus, it is evident that talc decreases the tensile modulus compared to pure epoxy, whereas the addition of WS enhances the tensile modulus in comparison to pure epoxy.

When comparing the results in terms of flexural strength, it is evident that the highest value is achieved in pure epoxy. In relation to flexural strength, the addition of talc to epoxy demonstrates a less adverse effect compared to WS. The contribution of WS further decreases the flexural strength in comparison to talc. In the combined use of WS and talc, talc exhibits a synergistic effect, positively influencing flexural strength. Upon examining the results for flexural modulus, it is noted that the sole addition of WS positively impacts the modulus compared to talc, whereas the sole addition of talc results in a modulus similar to that of epoxy. However, the simultaneous addition of talc and WS to the epoxy composite has a negative effect, leading to a reduction in the flexural modulus.

When comparing the results of the impact tests, it was observed that the highest impact resistance was achieved in pure epoxy, followed by epoxy composites filled with 3% WS and 3% talc, respectively. In epoxy composites where talc and WS are used together, the impact resistance value is lower compared to the other samples. This phenomenon is believed to be due to the increased interfacial incompatibility between WS, talc, and epoxy, leading to the creation of voids in the interfaces within the structure. It is thought that this is a result of the fibrous and foliated structure of talc [23].

### 3.5 Density and hardness measurement results

The graph depicting the results of the density and hardness tests is shown in Fig. 6. Pure epoxy exhibited a moderate hardness value and low density compared to the other samples. Among the blends, the sample labeled E97WS3, which had 3% walnut shell addition, achieved the highest hardness value at 78.8 shore D. Similarly, the sample coded as E97T3, with a 3% talc addition to the structure, demonstrated hardness values close to that of pure epoxy. This result is consistent with the phenomenon that talc increases the hardness in polymer composites [24]. Composite materials with high talc content may have lower hardness, while composites with

**Table 4** Experimental results of tensile and flexural testing on epoxy composites with varying weight percentages of WS and talc particles

Sample codes	Tensile properties			Flexural properties		
	Elastic modulus (MPa)	Tensile strength (MPa)	Elongation at break (%)	Elastic modulus (MPa)	Flexural strength (MPa)	Strain (%)
Pure epoxy	1104 ± 13.3	38.8 ± 1.0	4.4 ± 0.15	3032 ± 20.5	66.0 ± 0.82	3.1 ± 0.03
E97WS3	1190 ± 70.5	36.8 ± 0.3	3.9 ± 0.21	3370 ± 185.5	59.6 ± 2.79	3.1 ± 0.77
E97T3	1050 ± 23.3	35.4 ± 1.6	4.2 ± 0.42	3014 ± 51.5	60.5 ± 2.41	3.5 ± 0.57
E97WS1T2	1083 ± 99.8	34.5 ± 1.3	4.4 ± 0.33	2727 ± 154	57.7 ± 3.38	4.2 ± 0.20
E97WS2T1	1173 ± 66.3	36.1 ± 0.8	3.8 ± 0.34	2947 ± 34.8	59.9 ± 1.90	3.2 ± 0.65
E97WS1.5T1.5	1113 ± 45.6	35.0 ± 2.7	3.8 ± 0.44	2641 ± 79.0	56.8 ± 1.47	3.6 ± 0.75

Note: The values presented in the table are based on experimental testing and represent the average of multiple measurements

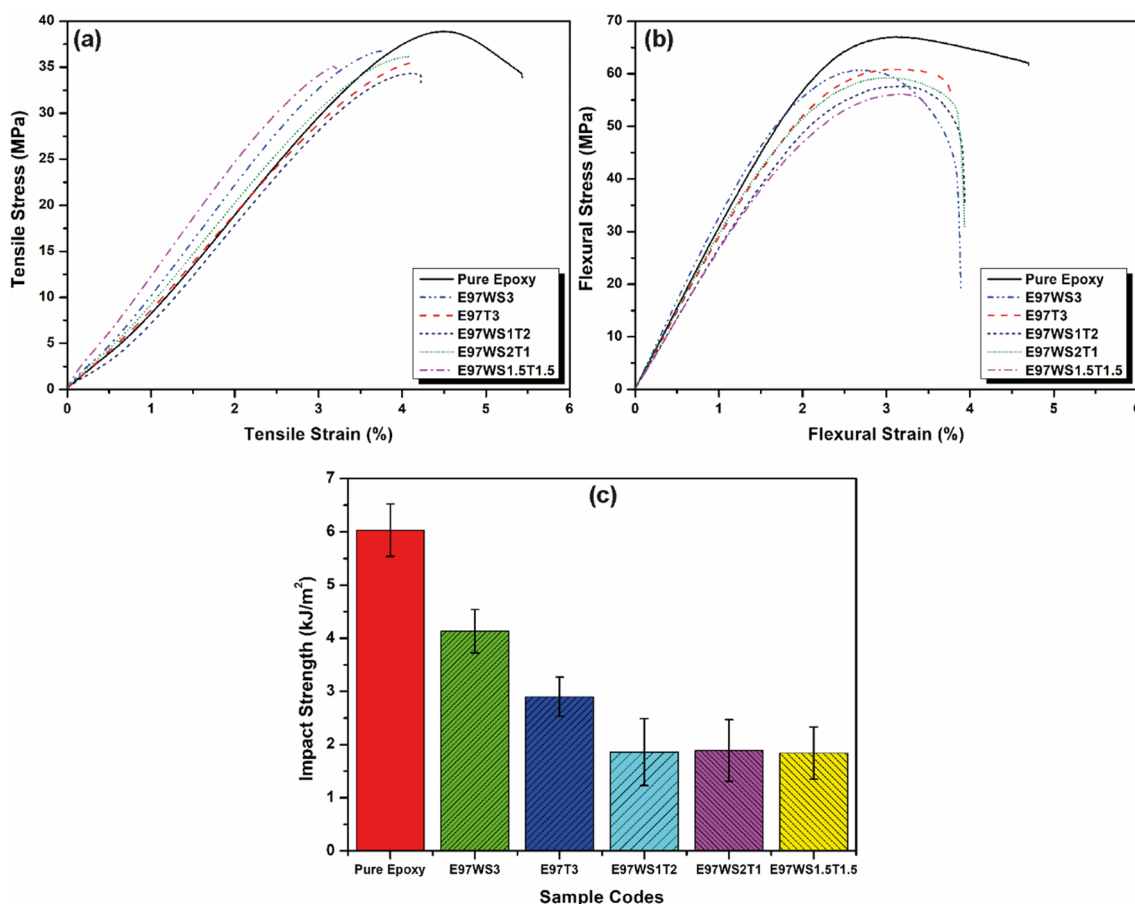


Fig. 5 Mechanical properties of pure epoxy and epoxy composites: **a** tensile stress, **b** flexural stress, and **c** impact strength

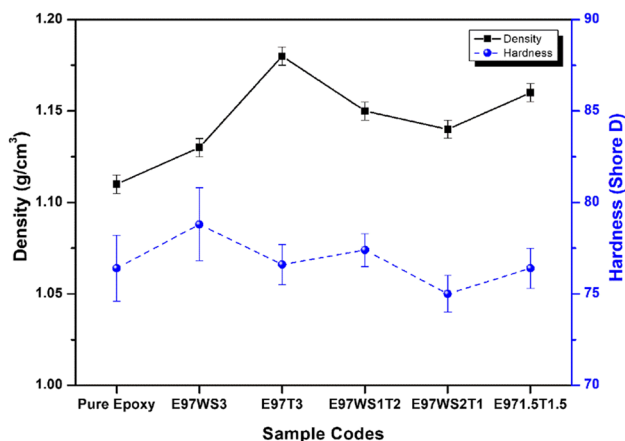


Fig. 6 Density and hardness of pure epoxy and epoxy composites

low talc content may provide higher hardness [22, 25]. The obtained results partially confirm this situation. Interestingly, despite being present in low proportions, talc filler had a more pronounced effect on the density of the composites compared to walnut shell filler. The higher density

of talc compared to walnut shell confirms this result. The higher density of talc compared to walnut shell is believed to contribute to this increase in overall density [26]. Samples where both talc and walnut shell were combined showcased a well-balanced profile in terms of hardness and density.

### 3.6 Water absorption test results

The water absorption capacities over time of both pure epoxy and epoxy composites are illustrated in Fig. 7. The water absorption capacity of pure epoxy is lower compared to that of epoxy composites. Epoxy composites with the addition of WS exhibit higher water absorption capacities than other composites. This is believed to be attributed to the hemicellulose present in WS. Degradation begins in all epoxy composites except pure epoxy after 216 h. Evaluations of epoxy composites indicate that as the WS filler ratio increases, the initially high-water absorption capacity starts to decrease after 144 h. This phenomenon can be associated with the hydrophilic nature of WS, limiting swelling in particles and preventing more water from entering the structure [27, 28].

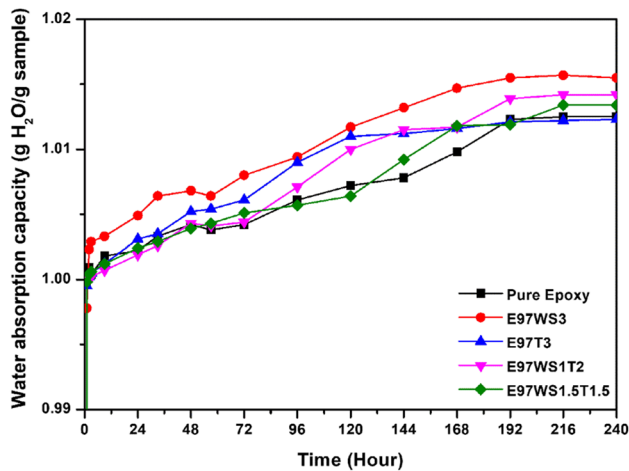


Fig. 7 Graphical comparison of water absorption capacity for pure epoxy and epoxy composites

### 3.7 Epoxy composites’ surface quality measurement results

The results of surface gloss and surface roughness measurements are presented in Table 5. Upon examining the results, it is observed that the surface gloss of pure epoxy composites falls within the glossy category. The addition of talc reduces glossiness and imparts a matte finish to the samples. The influence of WS on surface gloss is limited, and the surface gloss of epoxy composites is found to be at a semi-gloss level. A similar effect to the surface gloss situation is observed in the surface roughness values. The surface roughness values of samples with talc addition are higher compared to those with WS addition. The highest surface roughness value is measured in pure epoxy samples. This phenomenon can be explained by variations in the surface gloss and surface roughness of plastic parts, depending on factors such as mold surface, molding conditions, and filler materials.

### 3.8 Microstructure examination results

The size and geometry of ground walnut shell particles can be observed in Fig. 8a. Despite the rough surface, a significant number of particles exhibit a similar spherical shape (Fig. 8b) The WS type particle can be characterized by its shape, which is akin to that of a filler in this form. It is evident that WS has a fibrous structure, and the fiber arrangement appears similar on all sides (Fig. 8c) In general, walnut shells exhibit distinctive structures in their microarchitecture, characterized by simple pitted cell walls with caves or pores and a rolled sheets architecture [19].

On the surface of the pure epoxy specimen, as shown in Fig. 8d a relatively smooth, glassy, and homogeneous structure is observed with no signs of cracks or damage. However, as seen in Fig. 8e and f, in areas where voids formed during curing within the structure, the brittleness of the fracture surfaces becomes more pronounced. With the addition of WS (Fig. 8g) and talc (Fig. 8h) within the epoxy structure, the stress morphologies on the fracture surfaces become rougher. This alteration reduced the number of straight-line crack patterns progressing through the fracture morphology of the epoxy composite, roughening the crack surfaces, leading to more matrix deformation, and crack deflection. Consequently, the epoxy composites filled with WS and talc exhibited a lower mechanical resistance, breaking with significantly less energy under applied force compared to pure epoxy [18, 20]. The addition of WS along with talc to epoxy resulted in a rough structure and an irregular texture within the epoxy (Fig. 8i).

## 4 Conclusion

In this study, epoxy composites were successfully produced using the polymer casting method by incorporating low percentages (between 1 and 3%) of talc and WS. The influence of low filler ratios on the mechanical and thermal properties of epoxy composites was investigated. FT-IR spectra showed similar behavior in pure epoxy and walnut

Table 5 Surface roughness and gloss measurements

Sample codes	Surface roughness (Rz, μm)	Roughness improved efficiency (%)	Surface gloss (GU 60°)	Gloss improved efficiency (%)
Pure epoxy	16.0	–	85 (±6)	–
E97WS3	25.2	–157.5	80 (±3)	–6.0
E97T3	50.4	–315.0	70 (±7)	–21.5
E97WS1T2	40.6	–253.8	75 (±10)	–13.3
E97WS2T1	32.3	–201.9	78 (±2)	–9.0
E97WS1.5T1.5	40.2	–251.3	80 (±2)	–6.0

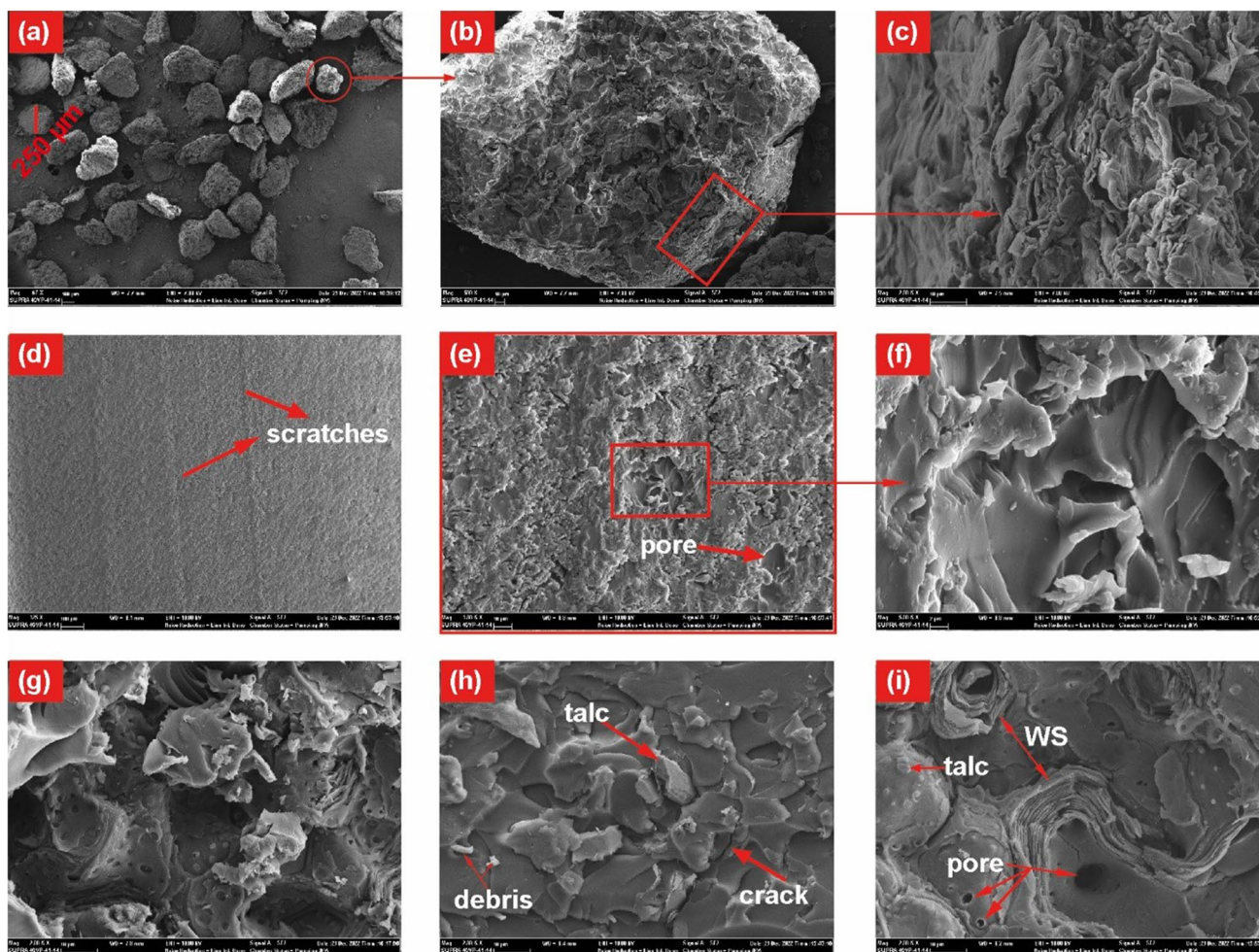


**Fig. 8** SEM micrograph shows a–c WS particles, d–f pure epoxy, g E97WS3, h E97T3, and i E97WS1.5T1.5

shell-filled composites, indicating shared molecular characteristics. In contrast, distinctive peaks in talc-filled composites confirmed the presence of talc in the epoxy matrix. DSC analyses revealed subtle thermal effects of additives. Talc slightly decreased the glass transition temperature ( $T_g$ ), suggesting increased flexibility, whereas walnut shell enhanced rigidity. Combining talc and walnut shell resulted in a balanced  $T_g$ , offering versatility for various temperature conditions. TGA analyses demonstrated the positive impact of walnut shell on thermal stability and the increased residue content contributed by talc. Talc reduced tensile strength but augmented hardness, whereas walnut shell positively influenced thermal stability and impact resistance. The combined use of talc and walnut shell exhibited a synergistic effect on  $T_g$ , resulting in a material with a harmonious combination of flexibility and rigidity. Density and hardness measurements indicated that talc increased hardness, while the simultaneous inclusion of talc and walnut shell achieved a balanced profile in terms

of hardness and density. Water absorption tests showcased the higher water absorption capacities of walnut shell composites due to their inherent hydrophilicity. Surface quality measurements unveiled the impact of additives on glossiness and surface roughness, with talc reducing glossiness and increasing roughness. Microstructure examination via SEM elucidated alterations in fracture surfaces, with both talc and walnut shell contributing to rougher morphologies, potentially influencing mechanical resistance. In conclusion, the use of talc and walnut shell as filler materials in epoxy composites, even at low percentages, offers a versatile material with adjustable thermal, mechanical, and surface properties.

**Author contribution** The determination of the parameters, interpretation of the results, and writing of the article were carried out by İdris Karagöz. The samples were prepared by Derya Mutlu and Aysu Çavusoğlu. Mechanical tests were conducted by Özgür Ceylan, and thermal tests were performed by Mithat Çelebi. All authors contributed to the writing of the article and the interpretation of the results.

**Funding** Open access funding provided by the Scientific and Technological Research Council of Türkiye (TÜBİTAK).

**Data availability** The raw data required to reproduce these findings can be obtained from the authors via email.

## Declarations

**Conflict of interest** The authors declare no competing interests.

**Open Access** This article is licensed under a Creative Commons Attribution 4.0 International License, which permits use, sharing, adaptation, distribution and reproduction in any medium or format, as long as you give appropriate credit to the original author(s) and the source, provide a link to the Creative Commons licence, and indicate if changes were made. The images or other third party material in this article are included in the article's Creative Commons licence, unless indicated otherwise in a credit line to the material. If material is not included in the article's Creative Commons licence and your intended use is not permitted by statutory regulation or exceeds the permitted use, you will need to obtain permission directly from the copyright holder. To view a copy of this licence, visit <http://creativecommons.org/licenses/by/4.0/>.

## References

- Zaghloul MMY, Zaghloul MMY, Fuseini M (2023) Recent progress in epoxy nanocomposites: corrosion, structural, flame retardancy and applications — a comprehensive review. In *Polymers Adv Technol* 34(11):3438–3472. <https://doi.org/10.1002/pat.6144>
- Wang H, Yuan J, Zhu Z, Yin X, Weng Y, Wang Z, Yang F, Zhan J, Wang H, Wang L (2021) High performance epoxy resin composites modified with multifunctional thiophene/phosphaphenanthrene-based flame retardant: excellent flame retardance, strong mechanical property and high transparency. *Compos Part B: Eng* 54:227. <https://doi.org/10.1016/j.compositesb.2021.109392>
- Balguri PK, Samuel DGH, Thumu U (2021) A review on mechanical properties of epoxy nanocomposites. *Mater Today: Proc* 44. <https://doi.org/10.1016/j.matpr.2020.09.742>
- Dinu R, Mija A (2020) Bio-based epoxy resins and composites from epoxidized linseed oil crosslinked with different cyclic anhydrides and their combination with lignin. *Cellulose Chem Technol* 54(9–10):925–938. <https://doi.org/10.35812/CelluloseChemTechnol.2020.54.89>
- Shin JH, Han GY, Kim HJ (2022) Latent, cross-linkable triazole platform on a carbon fiber surface for enhancing interfacial cross-linking within carbon fiber/epoxy composites. *ACS Omega* 7(15):12803–12815. <https://doi.org/10.1021/acsomega.2c00045>
- Bartoli M, Duraccio D, Faga MG, Piatti E, Torsello D, Ghigo G, Malucelli G (2022) Mechanical, electrical, thermal and tribological behavior of epoxy resin composites reinforced with waste hemp-derived carbon fibers. *Mater Sci* 57(31):14861–14876. <https://doi.org/10.1007/s10853-022-07550-9>
- Ding N, Wang X, Tian Y, Yang L, Chen H, Wang Z (2014) A renewable agricultural waste material for the synthesis of the novel thermal stability epoxy resins. *Polym Eng Sci* 54(12):2777–2784. <https://doi.org/10.1002/pen.23838>
- Mujtaba M, Fernandes Fraceto L, Fazeli M, Mukherjee S, Savassa SM, Araujo de Medeiros G, do Espírito Santo Pereira A, Mancini SD, Lipponen J, Vilaplana F (2023) Lignocellulosic biomass from agricultural waste to the circular economy: a review with focus on biofuels, biocomposites and bioplastics. *J Clean Prod*. <https://doi.org/10.1016/j.jclepro.2023.136815>
- Salasinska K, Barczewski M, Górny R, Kloziński A (2018) Evaluation of highly filled epoxy composites modified with walnut shell waste filler. *Polym Bull* 75(6):2511–2528. <https://doi.org/10.1007/s00289-017-2163-3>
- Singh VK (2015) Mechanical behavior of walnut (*Juglans L.*) shell particles reinforced bio-composite. *Sci Eng Compos Mater* 22(4). <https://doi.org/10.1515/secm-2013-0318>
- Zamani K, Kocaman S, Işık M, Soydal U, Özmeral N, Ahmetli G (2022) Water sorption thermal and fire resistance properties of natural shell-based epoxy composites. *J Applied Polymer Sci* 139(35). <https://doi.org/10.1002/app.52835>
- Sowińska-Baranowska A, Maciejewska M, Duda P (2022) The potential application of starch and walnut shells as biofillers for natural rubber (NR) composites. *Int J mol Sci* 23(14):7968. <https://doi.org/10.3390/ijms23147968>
- Barbu MC, Sepperer T, Tudor EM, Petutschnigg A (2020) Walnut and hazelnut shells: untapped industrial resources and their suitability in lignocellulosic composites. *Appl Sci (Switzerland)* 10(18):6340. <https://doi.org/10.3390/app10186340>
- Direk E, Ceylan M (2023) Effect of titanium dioxide and talc on the tensile strength of composite material. *Istanbul Ticaret Üniv Teknoloji ve Uygulamalı Bilimler Derg* 5(2):41–48. <https://doi.org/10.56809/icujtas.1136033>
- Tomasi JM, King JA, Krieg AS, Miskioglu I, Odegard GM (2018) Thermal, electrical, and mechanical properties of talc- and glass microsphere-reinforced cycloaliphatic epoxy composites. *Poly Compos* 39. <https://doi.org/10.1002/pc.24513>
- Le Huy CH, Thanh AT (2023) Study on fabricating epoxy coatings reinforced with iron oxide flakes and nano silica. *J Reinf Plast Compos* 42(13–14):724. <https://doi.org/10.1177/07316844231162562>
- Asil Kimya (2024) Talc 5 technical data sheet. <https://drive.google.com/file/d/1N4JRbHfPDqJI-aGXk6HhaFqbnbcn2dH0/view>. Accessed 01 Feb 2024
- Mutlu D, Karagöz İ, Sepetcioglu H, Tarim UA, Gurler O (2024) Synergizing electrical, mechanical, and radiation shielding properties of dendritic copper filled epoxy polymer composites. *Radiat Phys Chem* 216:111416. <https://doi.org/10.1016/j.radphyschem.2023.111416>
- Paçzkowski P (2023) Properties of eco-friendly composites based on post-consumer recycled resin filled with walnut shell powder. *Poly* 15(22):4389. <https://doi.org/10.3390/polym15224389>
- Ossman ME, Mansour MS, Fattah MA, Taha N, Kiros Y (2014) Peanut shells and talc powder for removal of hexavalent chromium from aqueous solutions. *Bulg Chem Commun* 46:629–639
- Onuchin DV, Sirotnin IS, Pavlova GA, Filatov SN, Kireev VV, Kerber ML, Gorbunova IY (2018) Features of curing of a diene epoxy oligomer modified with epoxyphosphazene. *Polym Sci Ser B*: 60(2):182–187. <https://doi.org/10.1134/S1560090418020069>
- Shnawa HA (2022) Studies on thermal properties and curing kinetics of talc-filled epoxy resin composite using differential scanning calorimetry. *Polym Bull* 79(12):11461–11478. <https://doi.org/10.1007/s00289-021-04012-1>
- Picard M, Thakur S, Misra M, Mielewski DF, Mohanty AK (2020) Biocarbon from peanut hulls and their green composites with biobased poly (trimethylene terephthalate) (PTT). *Sci Rep* 10(1):3310. <https://doi.org/10.1038/s41598-020-59582-3>
- Salasinska K, Barczewski M, Górny R, Kloziński A (2018) Evaluation of highly filled epoxy composites modified with walnut shell waste filler. *Polym Bull* 75(6):2511–2528. <https://doi.org/10.1007/s00289-017-2163-3>
- Tomasi JM, Krieg AS, Jensen NJ, Miskioglu I, King JA, Odegard GM (2019) Accelerated hygrothermal aging of talc/cycloaliphatic epoxy composites. *Polym Compos* 40(7):2946–2953. <https://doi.org/10.1002/pc.25131>
- Rathaur AS, Patel VK, Katiyar JK (2019) Tribo-mechanical properties of graphite/talc modified polymer composite bearing balls. *Mater Res Express* 7(1):015305

27. Mahmoud Y, Belhanché-Bensemra N, Safidine Z (2022) Impact of microcrystalline cellulose extracted from walnut and apricots shells on the biodegradability of poly (lactic acid). *Frontiers in Materials* 9:1005387. <https://doi.org/10.3389/fmats.2022.1005387>
28. Moo-Tun NM, Iñiguez-Covarrubias G, Valadez-Gonzalez A (2020) Assessing the effect of PLA, cellulose microfibers and CaCO<sub>3</sub> on the properties of starch-based foams using a factorial design. *Polym Testing* 86:106482

**Publisher's Note** Springer Nature remains neutral with regard to jurisdictional claims in published maps and institutional affiliations.